AIP | The Journal of Chemical Physics

Correlation between the variation in observed melting temperatures and structural motifs of the global minima of gallium clusters: An ab initio study

Anju Susan, Aniruddha Kibey, Vaibhav Kaware, and Kavita Joshi

Citation: J. Chem. Phys. **138**, 014303 (2013); doi: 10.1063/1.4772470
View online: http://dx.doi.org/10.1063/1.4772470
View Table of Contents: http://jcp.aip.org/resource/1/JCPSA6/v138/i1
Published by the American Institute of Physics.

Correlation between the variation in observed melting temperatures and structural motifs of the global minima of gallium clusters: An *ab initio* study

Anju Susan,[1] Aniruddha Kibey,[2] Vaibhav Kaware,[2] and Kavita Joshi[1]
[1]*CSIR-National Chemical Laboratory, Pune 411008, India*
[2]*Department of Physics, University of Pune, Pune 411007, India*

(Received 23 August 2012; accepted 3 December 2012; published online 3 January 2013)

We have investigated the correlation between the variation in the melting temperature and the growth pattern of small positively charged gallium clusters. Significant shift in the melting temperatures was observed for a change of only few atoms in the size of the cluster. Clusters with size between 31−42 atoms melt between 500–600 K whereas those with 46−48 atoms melt around 800 K. Density functional theory based first principles simulations have been carried out on Ga_n^+ clusters with $n = 31, \ldots, 48$. At least 150 geometry optimizations have been performed towards the search for the global minima for each size resulting in about 3000 geometry optimizations. For gallium clusters in this size range, the emergence of spherical structures as the ground state leads to higher melting temperature. The well-separated core and surface shells in these clusters delay isomerization, which results in the enhanced stability of these clusters at elevated temperatures. The observed variation in the melting temperature of these clusters therefore has a structural origin. © *2013 American Institute of Physics*. [http://dx.doi.org/10.1063/1.4772470]

I. INTRODUCTION

Finite size effects add to the complexity and richness of the already fascinating phenomenon of solid-liquid transition.[1–26] There are many glaring differences in the nature of *solid-like* to *liquid-like* transition at finite size compared to its bulk counterpart. One example of this is variation in the melting temperature (T_m) with the size of the cluster.[10,13,15] All elements have well-defined T_m in their bulk phase but clusters of the same element show a substantial variation in their melting temperatures, as observed in all the homogeneous systems studied so far.[10,13–15] For small Al and Ga clusters, the T_m varies as much as 400 K upon changing their size by a few atoms.[13,15]

Measured heat capacities of Ga clusters reveal many interesting observations.[13,16] First, all the clusters melt above their bulk melting temperatures ($T_{m(bulk)}$). The melting temperature for Ga in bulk phase is 303 K whereas all these clusters melt between 450 K to 850 K. Second, the *solid-like* to *liquid-like* transition is highly size dependent. Some clusters have a recognizable peak in their heat capacity curves, whereas some others do not show any signature of melting transition. The third observation is the variation in the T_m as a function of size of the cluster. The first two observations namely, higher than bulk melting temperatures and size sensitivity of melting transition, have been satisfactorily explained by employing the first principles simulations.[27,28] These simulations revealed that the bonding in small Ga clusters is covalent contrary to the mixture of covalent and metallic like bonding observed in α-gallium.[29] This change in the nature of bonding is the key to the elevated melting temperatures of gallium clusters.[27] Further, simulations have also revealed that magic melters have geometric origin.[28] However, the third feature, viz. variation in the melting temperatures is still an enigma and requires an explanation. Note that such a variation is a generic feature and is observed in all the clusters studied so far. For example, the variation in T_m is of order 100 K for Na clusters of size 55–357 atoms.[18] In the present work, we employ an *ab initio* molecular dynamics simulations to address the observed variation for Ga clusters in the size range 31−48.[13] This range can be divided into two groups. Clusters with sizes from 31−42 have their T_m in the range 500–600 K, whereas those with 46 to 48 atoms melt at about 800 K. Clearly, there is a difference of few hundred Kelvin when the size of the cluster varies by few atoms.

Initially, most of the simulations exploring the finite temperature behavior of small clusters employed empirical potentials.[2–8,24,30–33] These simulations brought out many interesting features such as dynamical coexistence of solid-liquid phases,[5–7] premelting,[8,31,34] and post-melting, which are peculiar to finite size systems. Our understanding about the nature of transition at finite size has been developed and enhanced by these early simulations. However, the experimental leap of measuring heat capacities of clusters with definite size also brought out the fact that classical molecular dynamics (CMD) with empirical potentials cannot reproduce the experimental results. The reason being, in most of the cases, the parameters used in these potentials are fitted such that one or more bulk properties could be reproduced. Obviously, these parameters fail to reproduce size specific properties of small clusters. For example, none of the CMD simulations with empirical potentials could reproduce the observed variation in melting temperature for free Na and Al clusters.[35–38] On the other hand, density functional theory based *ab initio* simulations[39–44] have reproduced these experimental results indicating that the use of *ab initio* methods is indispensable. It has been also demonstrated that the form of the classical potential influences, the structure of the ground state (GS).[30,45] On the other hand, more exact methods than DFT, such as CC,

CI combined with various search algorithms such as basin hopping or genetic algorithm lead to unaffordable computational cost even for small clusters with few atoms. Thus, DFT-based methods is a good bargain for accuracy and computational time.

There have been several attempts using DFT-based methods to understand the variation in the melting temperatures as a function of size of the cluster. Aguado and López investigated melting like transition in free Na clusters and indicated that structural effects can explain the variation in melting temperatures for these clusters.[46] Specifically, they bring out correlation between the maxima in the melting temperatures and high surface stability. Work done by Ghazi *et al.* on Na clusters also brings out the dependence of melting temperature on the structure of the most stable isomer.[47] Hock *et al.* investigated premelting and post-melting in Na clusters by comparing the finite temperature behavior of Na_{139} and Na_{147}.[48] It has been observed that for Na_{147}, the inner 13 atoms remain nearly fixed up to several tens of Kelvin above the T_m of outer two layers. Aguado and López have carried out simulations to understand the finite temperature properties of Al clusters on the basis of structure of the most stable isomer.[49–51] Their studies conclude that both geometric and electronic shell closing contribute to the variations in the cohesive energies and latent heats, but structural changes appear to be mainly responsible for the large variations in the melting temperatures with cluster size. Although, attempts have been made to understand the variation in T_m for Na and Al, there are very few investigations exploring the observed variation in Ga clusters. In our earlier work, we have investigated ten selected clusters in the above mentioned size range.[52] In this work, we investigate the growth pattern of positively charged gallium clusters with sizes between 31−48 atoms and its repercussion(s) on their finite temperature behavior. Considering the continuous range has many advantages over exploring selected sizes, such as, it reduces the chances of landing on a wrong structural motif. Further, for most of the sizes the charged clusters have a lowest energy structure different than their neutral counterpart which explains the data better.[52] We demonstrate that the variation in melting temperatures have a structural origin. Change in the structural motif correlates well with variation in the melting temperatures. Further, the clusters having the global minima dominated with the formation of planes have lower melting temperatures compared to those with spherical structure (with distinct core and surface shells).

The paper is organized as follows. In Sec. II, we describe the computational details. The results and discussion are presented in Sec. III and the conclusions are drawn in Sec. IV.

II. COMPUTATIONAL DETAILS

The structures were optimized using Born-Oppenheimer molecular dynamics based on the Kohn-Sham formulation of density functional theory. The interactions between the ion and valence electrons are described using projector augmented wave (PAW) potentials,[53] with the generalized gradient approximation (GGA), and the Perdew-Burke-Ernzerhof (PBE) exchange-correlation functional[54] as implemented in the Vienna *Ab initio* Simulation package (VASP).[55–58] This level of theory is sufficient to reproduce experimental melting temperatures as shown by many simulations.[39,59] The size of the simulation box is 25 Å, which is found to provide sufficient convergence in the total electronic energy. The search for the global minima was a multi-step process. We begin by optimizing the previously published geometries for neutral Ga[52] and Al clusters.[60,61] We quenched all these geometries for Ga by appropriately scaling the bondlengths. We also quenched the geometries obtained by employing empirical potentials.[62] The lowest energy structure within all such quenches is then taken as a starting point for the next level of search for the GS. Since the melting temperatures were already known from the experiments,[13] all clusters were maintained at three different temperatures near their respective T_m for few hundred pico seconds (300 ps or more). Structures for local optimization were then selected from these high temperature melt. Several geometries were also constructed by adding (removing) atoms to smaller (larger) clusters. We have carried out at least 150 geometry optimizations per system, which results into about 3000 geometry optimizations for the whole series. The structure with the lowest energy is treated as the global minima found within this search.

Since we are searching for the entire series, it improves our initial guess for the ground state structure. For example, the GS for 32−34 are constructed by adding atoms to the GS of 31, and the resulting structures are lowest in energy within all the optimized structures for these sizes. For 35 atom cluster, the structure constructed from Ga_{31}^+ GS is 0.16 eV higher in energy, marking the change of structural motif. The other advantage of working with whole series is that the chance of landing on a completely different structural motif from the GS reduces when we consider the evolutionary trend. To the best of our knowledge, there is no systematic study available on the evolutionary pattern of the charged clusters of gallium in the given range. However, there are few studies available for neutral as well as charged gallium clusters with smaller sizes.[63–68] Comparing the GS for available neutral clusters also underlines the need to simulate charged clusters to understand the experimental observations better.

III. RESULTS AND DISCUSSION

First, we describe the ground state structures. As mentioned earlier, we have about 150 distinct isomers for each size. In Figs. 1–3, we show the most stable isomer for 31 to 48 atom cation clusters. We have grouped these isomers into three different classes. From 31−39, the GS are dominated by formation of planes, and are shown in Fig. 1. From 40−42 is the transition region, shown in Fig. 2, and 43–48, whose GS are dominated by spherical polyhedra with distinct core, shown in Fig. 3. It is evident from Fig. 1 that the most stable isomers for Ga_{31}^+ to Ga_{39}^+ are dominated by the formation of planes (as discussed later). A different view, where the parallel planes are evident for three representative systems is labeled as "a" and is shown in the last column of the figure. The GS for Ga_{31}^+ is a three layered structure with A–B–A packing (see **31a** in Fig. 1). Up to 34 atom cluster, the structural motif for the GS is same as that of Ga_{31}^+. However,

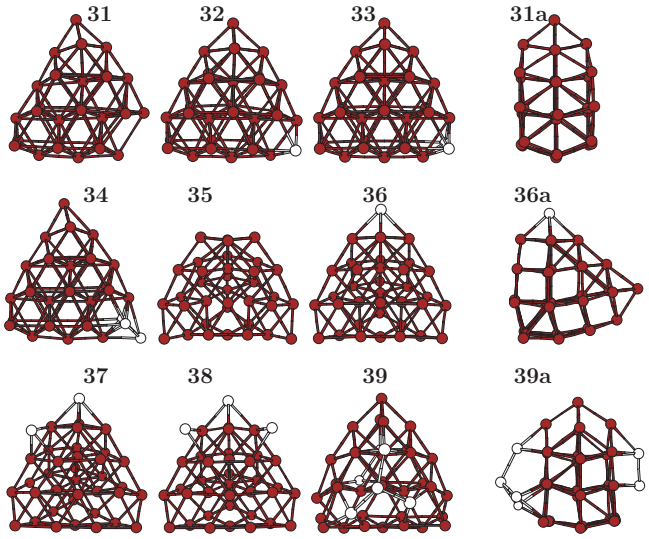

FIG. 1. The most stable isomers for Ga_{31}^{+} to Ga_{39}^{+} are shown. The last column gives a different view obtained by rotating the cluster and labeled as **a**. All the geometries are dominated by formation of planes. Ga_{31}^{+} is considered as the base structure till 34. Ga_{35}^{+} is considered as the reference structure till 38. Atoms shown in white represent additions to the base structure. Ga_{39}^{+} has same structural motif as that of Ga_{31}^{+} and the atoms in white indicate additions over Ga_{33}^{+}.

depending upon the position of the ad atom (shown by white atoms in the Fig. 1), the packing varies from A–B–A to A–B–C. At 35, the structural motif changes to distorted decahedral fragment (DDF) and is accompanied by change in the slope of T_m at this size (see Fig. 6). This structural motif remains the same till 38. The ad atoms are shown in white for larger clusters up to 38 atoms. The GS for 39 atom cluster has same structural motif as that of Ga_{33}^{+} and the atoms shown in white are addition to Ga_{33}^{+}. The T_m for all these clusters are between 500 K to 600 K. Next, we show the most stable structures for Ga_{40}^{+} to Ga_{42}^{+} in Fig. 2. These structures indicate transition of the GS towards spherical shape. As can be seen from the figure, a part of the cluster is still dominated by formation of planes and the other part tends to be more spherical. The GS for clusters having spherical geometries are shown in Fig. 3. It is interesting to note that the GS for all these clusters have distinct core. For clarity, the core atoms are shown with different (red) color. As we will see later, the building up of core plays a crucial role in stabilizing the cluster at higher temperatures. To summarize, the GS is dominated by planes till 39 and around 43, the GS becomes spherical with distinct core formation.

This structural transition is brought out more clearly by shape analysis, shown in Fig. 4. To demonstrate that atoms are

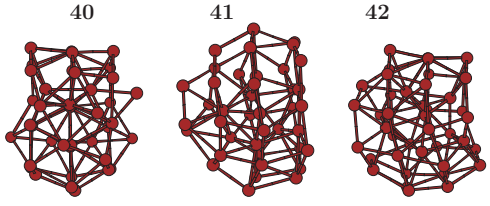

FIG. 2. The most stable isomers for Ga_{40}^{+} to Ga_{42}^{+} are shown. The transition from elongated structures towards spherical structure is evident.

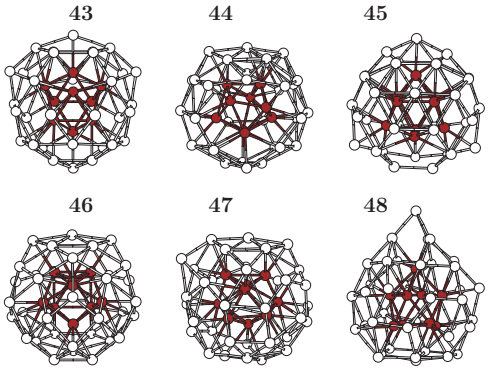

FIG. 3. The most stable isomers for Ga_{43}^{+} to Ga_{48}^{+} are shown. Clearly, all these structures are spherical with distinct core and surface shells. For clarity, the core atoms are shown in red.

mainly distributed in planes up to 39, we have calculated regression plane for the set of atoms associated with distinct planes. The distance between the atoms and the respective regression plane fitted to these atoms is shown in Fig. 4(a). Thus, for Ga_{31}^{+} to Ga_{34}^{+} there are three sets of atoms, each set representing a plane. For 35 to 38, four regression planes could be fitted. The deviation of atoms from regression plane ranged between 0.002–0.12 Å up to size 34 and less than 10% of plane separation (~3 Å) for larger clusters till size 39. In order to verify the spherical shell formation among some of the clusters, we calculated the distance of each atom from the x, y, and z axes (along planes y-z, z-x, x-y, respectively), and plotted it against the x, y, and z co-ordinates, respectively, as shown in Fig. 4(b). For the better representation of the data, the distances were given the sign of y, z, and x co-ordinates, respectively. For a spherical cluster (e.g., Ga_{46}^{+}), for each axis, the atoms near the poles are closest to the given axis, while towards the center they move away from the axis progressively. Thus, for a cluster forming spherical shell, the above gives a circular distribution of distances along each axis. Fig. 4(b) shows two concentric circles for Ga_{46}^{+} confirming the existence of distinct and well-separated core and surface shells. On the contrary, other clusters show scattered distribution indicating absence of such shells.

Thus, we have demonstrated that the GS can be broadly classified into two different structural motifs. Clusters with sizes up to 39 have "planes" as a part of GS, whereas clusters with high T_m have spherical structures with distinct core and surface shells. Now we select one cluster from each of the class to demonstrate how different structural motifs affect the finite temperature behavior. In Fig. 5, we show the distribution of atoms with respect to the center of mass (COM) of the cluster for the two representative sizes, Ga_{36}^{+} and Ga_{46}^{+}. For Ga_{36}^{+}, there are 4 core atoms, and the rest 32 atoms form its surface. However, the surface atoms are distributed in subshells spread over 2.5 Å. Contrary to this, for Ga_{46}^{+}, there are two distinct shells centered about the COM. The development of this distinct core and surface shell is one of the key factors in determining the finite temperature behavior of these clusters, as we will demonstrate later.

Fig. 6. shows the number of bonds between internal atoms (or core atoms) as a function of cluster size. It indicates

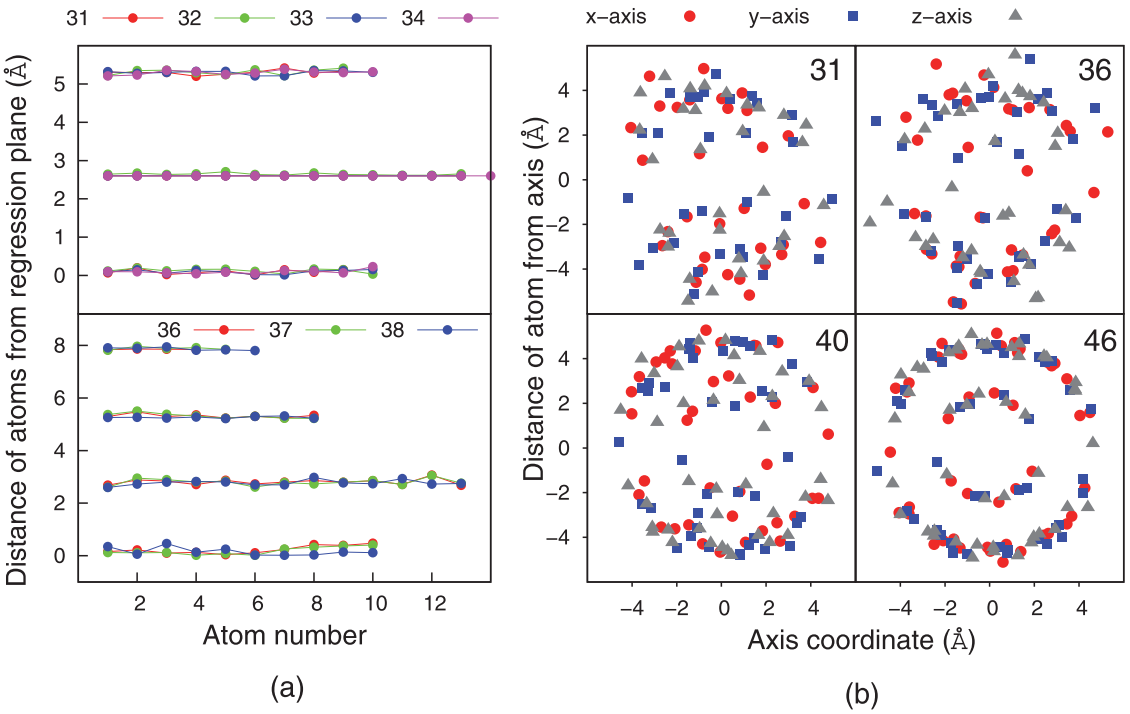

FIG. 4. (a) Perpendicular distance of each atom from the fitted regression plane, showing almost planar arrangement of atoms, for sizes indicated. Separation between planes is taken as 2.6 for plotting. (b) Plot of distance of each atom, along y-z/z-x/x-y plane, against the x/y/z axis coordinate, respectively, for sizes 31, 36, 40, and 46. For size 46, the graph signifies that core-shell type formation is symmetrically seen along all the three axes, while others show a scatter.

a substantial increase in the number of bonds between core atoms, upon change of the structural motif from "planar" to "spherical." For clusters in class I (i.e., clusters with low T_m), the number of bonds within internal atoms is less than one per atom, whereas for spherical clusters there are about 2 bonds per core atom. Thus, the spherical clusters have a strongly connected core. This strongly connected core delays the isomerization in these clusters as can be seen from Fig. 7, where we show different families of isomers and their relative energies with respect to the GS. We have identified different families of isomers such as three layered structures with A–B–A or A–B–C packing, distorted decahedral fragments (DDF), DDF with surface, or edge atoms missing from the base structure and located as caps (DDFs or DDFe), spherical structures with and without distinct core (Sph), and finally the disordered isomers. Although, these isomer families are shown as a point on the graph, they span an energy range with the starting point shown in the figure. For example, for Ga_{45}^+, the isomer family Sph shown only as a black circle at 0.51 eV, has its isomers extending in energy from 0.51 eV up to 1.17 eV. Similarly, other classes have their energies extending upwards from the point shown in the figure. For all clusters smaller than 39, the first isomer family starts at 0.2 eV or less above the base energy, whereas for clusters larger than 44, the first isomer family begins at 0.5 eV or above. Thus, the

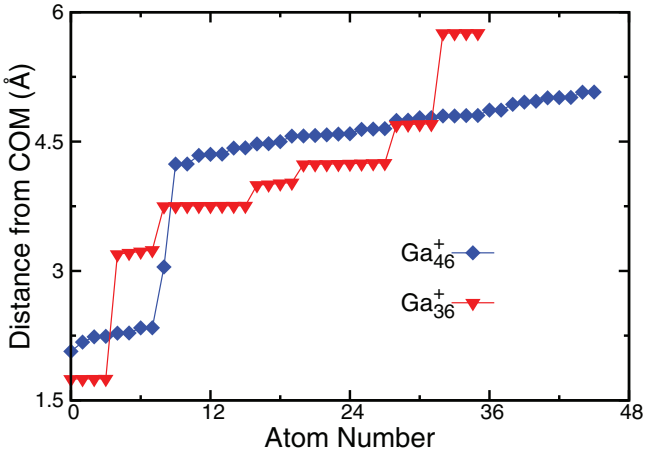

FIG. 5. Distribution of atoms from the center of mass of the cluster. For Ga_{46}^+, there are two distinct shells, which are absent in Ga_{36}^+.

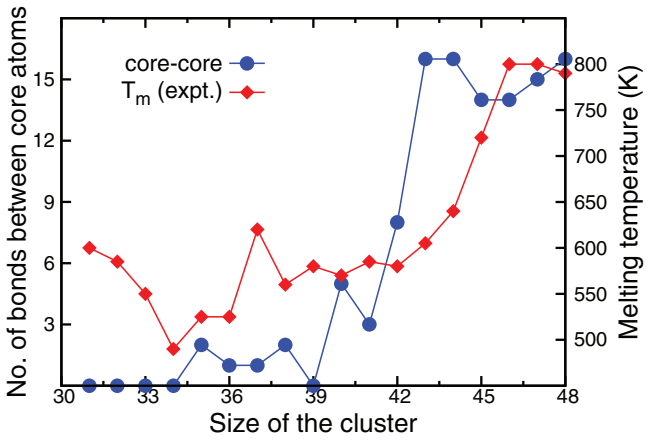

FIG. 6. The number of bonds between core atoms (blue) as a function of cluster size. Significant increase in the number of bonds has been observed for spherical clusters having elevated melting temperatures. Experimentally measured T_m (red) from Ref. 13 are also shown.

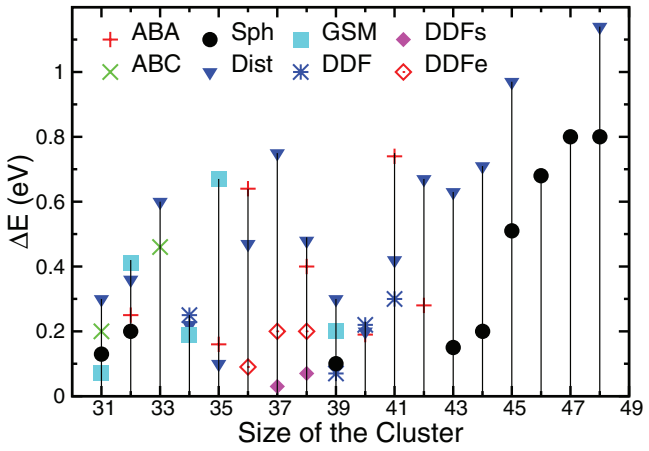

FIG. 7. The energy difference with respect to the GS for different families of isomers as a function of cluster size. **ABA** and **ABC**: three layered structures with different packing types, **DDF**: distorted decahedral fragment, **Sph**: spherical structures without core and surface distinction, **GSM**: geometries with minor changes to the GS but with same structural motif, **DDFs**: DDF structural motif with one of the surface atoms displaced, **DDFe**: DDF structural motif with one of the edge atoms displaced. Note that for clusters with high T_m, the energy difference between the GS and the first isomer family is about 0.7 eV or higher, whereas for clusters having low T_m, occurrence of various isomer families is observed at much lower energy difference.

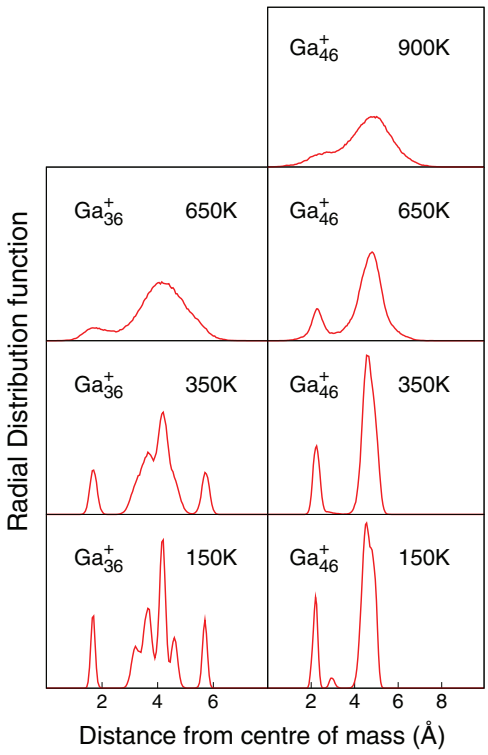

FIG. 8. Distribution of atoms about the center of mass of the cluster for Ga_{36}^+ and Ga_{46}^+ at various temperatures. The clusters are maintained at these temperatures for 180 ps. Interestingly, for Ga_{36}^+ at 650 K, the absence of well-separated shells indicates that the cluster is already in *liquid-like* state whereas, Ga_{46}^+ exhibits the same behavior at 900 K.

appearance of first isomer family at as high as 0.5 eV also indicates delayed isomerization, which is one of the first steps towards melting of the cluster.

To understand the effect of distinct core-shell structure, we have also simulated these two clusters at three different temperatures. We have selected Ga_{36}^+ and Ga_{46}^+ clusters with respective T_m being 550 K and 800 K. Both clusters are kept at 150 K, 350 K, 650 K for 180 ps each. Ga_{46}^+ is also maintained at 900 K, i.e., slightly above its T_m for 180 ps. In Fig. 8, we show the radial distribution of atoms for Ga_{36}^+ and Ga_{46}^+ about the COM of the cluster computed over the last 150 ps. For a 36 atom cluster, at 150 K, there are three distinct shells. The first peak represents 4 internal atoms, while the last peak represents 4 vertex atoms. The in-between peaks are due to the remaining 28 surface atoms, which have already merged into each other indicating the initiation of inter-shell diffusion. The separate peaks for internal and vertex atoms indicate that the atoms belonging to these shells are still confined. As the temperature rises further, at 350 K the middle and the last shell are on the verge of merging but the first shell is still unaltered except the expected thermal broadening. However, at 650 K all the shells have lost their identity and the cluster is in liquid-like state. Comparing this behavior with that of 46 atom cluster, at 150 K there are only two shells present, the core and the surface. With increasing temperature, although thermal broadening is observed, atoms are not diffusing from one shell to another. At 650 K as well, the cluster retains the existence of two separate shells although, inter shell diffusion is observed. The cluster is in a liquid-like state around 900 K as evident from the radial distribution function at that temperature where the shells have lost their separate identity.

Melting in general and specifically in the finite size systems is a complex phenomenon. From all investigations that have been done so far, experimentally as well as via simulations, it has been clearly brought out that there are many factors that influence the melting transition. Electronic shell closing, geometric stability, shape, surface area are a few of the most important factors. Although it is known that many factors contribute to the finite temperature stability of a cluster, their exact dependence is not yet completely understood. The contribution of these factors also varies with the size of the cluster. Here, we brought out the effect of the structural transition of the GS on the melting temperatures of clusters. We also point out factors contributing to the higher stability of cluster at elevated temperatures. Clusters with spherical geometries have higher T_m owing to the stability of core and surface at high temperatures. The cluster is considered to be melted when atoms can freely move around in the cluster. In other words, till the cluster retains the separate identity of its shells, it is not in a liquid like state. The main deciding factor for elevated T_m, for the range studied here, is the shell formation. The GS for clusters with elevated melting temperatures have two distinct shells. The well-separated shells also lead to higher connectivity within the atoms of each shell. This in turn leads to the stability of shells at higher temperatures and in general higher melting temperatures for the cluster. On the other hand, for clusters with no shell formation, it has been also noted that the internal atoms are rather weakly connected with each other with interatomic distance more than 2.8 Å while the shortest bond in the cluster is about 2.55 Å. It is easier for atoms to diffuse through the shells, which are not well

separated, since at slightly higher temperatures, their vibrational amplitude will have same displacements as the distance between two near by shells.

IV. CONCLUSION

The *ab initio* density functional simulations have been employed to search for the putative global minima of positively charged gallium clusters Ga_n^+ with $n = 31, \ldots, 48$. We clearly bring out the factors responsible for observed shift in the melting temperature of these clusters. Our investigations demonstrate that there is a correlation in the variation of the melting temperature and the structural motif of the global minima. Emergence of spherical structures as the ground state leads to higher melting temperature. The well-separated core and surface shells in these clusters delay isomerization, which results in an enhanced stability of these clusters at elevated temperatures. Thus, a change in the structural motif of the GS correlates well with the observed shift in the T_m.

ACKNOWLEDGMENTS

K.J. and A.S. would like to acknowledge the Center of Excellence for Scientific Computing for the in-part funding to the project. CDAC-Pune and IUAC-Delhi are acknowledged for providing the super-computing facility. A.S. acknowledges CSIR for financial support.

[1]T. L. Hill, *Thermodynamics of Small Systems* (Courier-Dover, 1994), Vols. I and II.
[2]R. S. Berry, "Introductory lecture. Clusters, melting, freezing and phase transitions," J. Chem. Soc., Faraday Trans. **86**(13), 2343–2349 (1990).
[3]R. S. Berry, "Melting, freezing and other peculiarities in small systems," Phase Transitions **24–26**(1), 259–270 (1990).
[4]J. P. Rose and R. S. Berry, "$(KCl)_{32}$ and the possibilities for glassy clusters," J. Chem. Phys. **98**(4), 3262–3274 (1993).
[5]H.-P. Cheng, X. Li, R. L. Whetten, and R. S. Berry, "Complete statistical thermodynamics of the cluster solid-liquid transition," Phys. Rev. A **46**(2), 791–800 (1992).
[6]R. E. Kunz and R. S. Berry, "Coexistence of multiple phases in finite systems," Phys. Rev. Lett. **71**(24), 3987–3990 (1993).
[7]D. J. Wales and R. S. Berry, "Coexistence in finite systems," Phys. Rev. Lett. **73**(21), 2875–2878 (1994).
[8]H.-P. Cheng and R. S. Berry, "Surface melting of clusters and implications for bulk matter," Phys. Rev. A **45**(11), 7969–7980 (1992).
[9]D. J. Wales and J. P. K. Doye, "Coexistence and phase separation in clusters: From the small to the not-so-small regime," J. Chem. Phys. **103**(8), 3061–3070 (1995).
[10]B. von Issendorff, H. Haberland, M. Schmidt, and R. Kusche, "Irregular variations in the melting point of size-selected atomic clusters," Nature (London) **393**(6682), 238–240 (1998).
[11]A. Aguado and M. F. Jarrold, "Melting and freezing of metal clusters," Annu. Rev. Phys. Chem. **62**(1), 151–172 (2011).
[12]M. Schmidt, R. Kusche, T. Hippler, J. Donges, W. Kronmüller, B. von Issendorff, and H. Haberland, "Negative heat capacity for a cluster of 147 sodium atoms," Phys. Rev. Lett. **86**(7), 1191–1194 (2001).
[13]G. A. Breaux, D. A. Hillman, C. M. Neal, R. C. Benirschke, and M. F. Jarrold, "Gallium cluster 'magic melter,'" J. Am. Chem. Soc. **126**(28), 8628–8629 (2004).
[14]G. A. Breaux, C. M. Neal, B. Cao, and M. F. Jarrold, "Melting, premelting, and structural transitions in size-selected aluminum clusters with around 55 atoms," Phys. Rev. Lett. **94**(17), 173401 (2005).
[15]C. M. Neal, A. K. Starace, and M. F. Jarrold, "Ion calorimetry: Using mass spectrometry to measure melting points," J. Am. Soc. Mass Spectrom. **18**(1), 74–81 (2007).
[16]G. A. Breaux, R. C. Benirschke, T. Sugai, B. S. Kinnear, and M. F. Jarrold, "Hot and solid gallium clusters: Too small to melt," Phys. Rev. Lett. **91**(21), 215508 (2003).
[17]M. Schmidt, R. Kusche, W. Kronmüller, B. von Issendorff, and H. Haberland, "Experimental determination of the melting point and heat capacity for a free cluster of 139 sodium atoms," Phys. Rev. Lett. **79**(1), 99–102 (1997).
[18]M. Schmidt and H. Haberland, "Phase transitions in clusters," C. R. Phys. **3**(3), 327–340 (2002).
[19]F. Chirot, P. Feiden, S. Zamith, P. Labastie, and J.-M. L'Hermite, "A novel experimental method for the measurement of the caloric curves of clusters," J. Chem. Phys. **129**(16), 164514 (2008).
[20]C. M. Neal, A. K. Starace, and M. F. Jarrold, "Melting transitions in aluminum clusters: The role of partially melted intermediates," Phys. Rev. B **76**(5), 054113 (2007).
[21]M. F. Jarrold, B. Cao, A. K. Starace, C. M. Neal, and O. H. Judd, "Metal clusters that freeze into high energy geometries," J. Chem. Phys. **129**(1), 014503 (2008).
[22]A. A. Shvartsburg and M. F. Jarrold, "Solid clusters above the bulk melting point," Phys. Rev. Lett. **85**(12), 2530–2532 (2000).
[23]G. A. Breaux, C. M. Neal, B. Cao, and M. F. Jarrold, "Tin clusters that do not melt: Calorimetry measurements up to 650 K," Phys. Rev. B **71**(7), 073410 (2005).
[24]R. S. Berry, J. Jellinek, and G. Natanson, "Melting of clusters and melting," Phys. Rev. A **30**(2), 919–931 (1984).
[25]Y. J. Lee, E.-K. Lee, S. Kim, and R. M. Nieminen, "Effect of potential energy distribution on the melting of clusters," Phys. Rev. Lett. **86**(6), 999–1002 (2001).
[26]H. Haberland, T. Hippler, J. Donges, O. Kostko, M. Schmidt, and B. von Issendorff, "Melting of sodium clusters: Where do the magic numbers come from?," Phys. Rev. Lett. **94**(3), 035701 (2005).
[27]S. Chacko, K. Joshi, D. G. Kanhere, and S. A. Blundell, "Why do gallium clusters have a higher melting point than the bulk?," Phys. Rev. Lett. **92**(13), 135506 (2004).
[28]K. Joshi, S. Krishnamurty, and D. G. Kanhere, ""Magic melters" have geometrical origin," Phys. Rev. Lett. **96**(13), 135703 (2006).
[29]X. G. Gong, G. L. Chiarotti, M. Parrinello, and E. Tosatti, "α-gallium: A metallic molecular crystal," Phys. Rev. B **43**(17), 14277–14280 (1991).
[30]J. P. K. Doye, D. J. Wales, and R. S. Berry, "The effect of the range of the potential on the structures of clusters," J. Chem. Phys. **103**(10), 4234–4249 (1995).
[31]Z. B. Güvenç and J. Jellinek, "Surface melting in Ni_{55}," Z. Phys. D: At., Mol. Clusters **26**(1), 304–306 (1993).
[32]J. Jellinek and I. L. Garzón, "Structural and dynamical properties of transition metal clusters," Z. Phys. D: At., Mol. Clusters **20**(1), 239–242 (1991).
[33]N. Ju and A. Bulgac, "Finite-temperature properties of sodium clusters," Phys. Rev. B **48**(4), 2721–2732 (1993).
[34]F. Calvo and F. Spiegelmann, "Geometric size effects in the melting of sodium clusters," Phys. Rev. Lett. **82**(11), 2270–2273 (1999).
[35]F. Calvo and F. Spiegelmann, "Mechanisms of phase transitions in sodium clusters: From molecular to bulk behavior," J. Chem. Phys. **112**(6), 2888–2908 (2000).
[36]E. G. Noya, J. P. K. Doye, and F. Calvo, "Theoretical study of the melting of aluminum clusters," Phys. Rev. B **73**(12), 125407 (2006).
[37]F. Calvo and F. Spiegelman, "On the premelting features in sodium clusters," J. Chem. Phys. **120**(20), 9684–9689 (2004).
[38]J. A. Reyes-Nava, I. L. Garzón, and K. Michaelian, "Negative heat capacity of sodium clusters," Phys. Rev. B **67**(16), 165401 (2003).
[39]S. Chacko, D. G. Kanhere, and S. A. Blundell, "First principles calculations of melting temperatures for free Na clusters," Phys. Rev. B **71**(15), 155407 (2005).
[40]A. Rytkönen, H. Häkkinen, and M. Manninen, "Melting and multipole deformation of sodium clusters," Eur. Phys. J. D **9**, 451 (1999).
[41]K. Manninen, A. Rytkönen, and M. Manninen, "Influence of electronic and geometric properties on melting of sodium clusters," Eur. Phys. J. D **29**(1), 39–47 (2004).
[42]S. Zorriasatein, M.-S. Lee, and D. G. Kanhere, "Electronic structures, equilibrium geometries, and finite-temperature properties of $Na_n (n = 39, \ldots, 55)$ from first principles," Phys. Rev. B **76**(16), 165414 (2007).
[43]A. Aguado and J. M. López, "Small sodium clusters that melt gradually: Melting mechanisms in Na_{30}," Phys. Rev. B **74**(11), 115403 (2006).
[44]M.-S. Lee and D. G. Kanhere, "Effects of geometric and electronic structure on the finite temperature behavior of Na_{58}, Na_{57}, and Na_{55} cluster," Phys. Rev. B **75**(12), 125427 (2007).
[45]Z. Ma, W. Cai, and X. Shao, "Impact of different potentials on the structures and energies of clusters," J. Comput. Chem. **32**(14), 3075–3080 (2011).

[46]A. Aguado and J. M. López, "Anomalous size dependence in the melting temperatures of free sodium clusters: An explanation for the calorimetry experiments," Phys. Rev. Lett. **94**(23), 233401 (2005).
[47]S. M. Ghazi, S. Zorriasatein, and D. G. Kanhere, "Building clusters atom-by-atom: From local order to global order," J. Phys. Chem. A **113**(12), 2659–2662 (2009).
[48]C. Hock, C. Bartels, S. Straßburg, M. Schmidt, H. Haberland, B. von Issendorff, and A. Aguado, "Premelting and postmelting in clusters," Phys. Rev. Lett. **102**(4), 043401 (2009).
[49]A. Aguado and J. M. López, "First-principles structures and stabilities of Al_N^+ (N = 4662) clusters," J. Phys. Chem. B **110**(29), 14020–14023 (2006).
[50]A. K. Starace, C. M. Neal, B. Cao, M. F. Jarrold, A. Aguado, and J. M. Lopez, "Correlation between the latent heats and cohesive energies of metal clusters," J. Chem. Phys. **129**(14), 144702 (2008).
[51]A. K. Starace, C. M. Neal, B. Cao, M. F. Jarrold, A. Aguado, and J. M. Lopez, "Electronic effects on melting: Comparison of aluminum cluster anions and cations," J. Chem. Phys. **131**(4), 044307 (2009).
[52]S. Krishnamurty, K. Joshi, S. Zorriasatein, and D. G. Kanhere, "Density functional analysis of the structural evolution of Ga_n (n = 30–55) clusters and its influence on the melting characteristics," J. Chem. Phys. **127**(5), 054308 (2007).
[53]P. E. Blöchl, "Projector augmented-wave method," Phys. Rev. B **50**(24), 17953–17979 (1994).
[54]J. P. Perdew, K. Burke, and M. Ernzerhof, "Generalized gradient approximation made simple," Phys. Rev. Lett. **77**(18), 3865–3868 (1996).
[55]G. Kresse and J. Hafner, "*Ab initio* molecular-dynamics simulation of the liquid-metal-amorphous-semiconductor transition in germanium," Phys. Rev. B **49**(20), 14251–14269 (1994).
[56]G. Kresse and J. Furthmller, "Efficiency of *ab initio* total energy calculations for metals and semiconductors using a plane-wave basis set," Comput. Mater. Sci. **6**(1), 15–50 (1996).
[57]G. Kresse and J. Furthmüller, "Efficient iterative schemes for *ab initio* total-energy calculations using a plane-wave basis set," Phys. Rev. B **54**(16), 11169–11186 (1996).
[58]G. Kresse and D. Joubert, "From ultrasoft pseudopotentials to the projector augmented-wave method," Phys. Rev. B **59**(3), 1758–1775 (1999).
[59]J. Kang, S.-H. Wei, and Y.-H. Kim, "Origin of the diverse melting behaviors of intermediate-size nanoclusters: Theoretical study of Al_n (n = 5158, 64)," J. Am. Chem. Soc. **132**(51), 18287–18291 (2010).
[60]C. M. Neal, A. K. Starace, M. F. Jarrold, K. Joshi, S. Krishnamurty, and D. G. Kanhere, "Melting of aluminum cluster cations with 3148 atoms: Experiment and theory," J. Phys. Chem. C **111**(48), 17788–17794 (2007).
[61] L. Ma, B. v. Issendorff, and A. Aguado, "Photoelectron spectroscopy of cold aluminum cluster anions: Comparison with density functional theory results," J. Chem. Phys. **132**, 104303 (2010); see supplementary material at http://dx.doi.org/10.1063/1.3352445 for geometry coordinates.
[62]See http://www-wales.ch.cam.ac.uk/CCD.html for coordinates of geometries optimized using empirical potentials.
[63]R. O. Jones, "Simulated annealing study of neutral and charged clusters: Al_n and Ga_n," J. Chem. Phys. **99**(2), 1194–1206 (1993).
[64]B. Song and P. L. Cao, "Evolution of the geometrical and electronic structures of Ga_n (n = 2–26) clusters: A density-functional theory study," J. Chem. Phys. **123**(14), 144312 (2005).
[65]S. Krishnamurty, S. Chacko, D. G. Kanhere, G. A. Breaux, C. M. Neal, and M. F. Jarrold, "Size-sensitive melting characteristics of gallium clusters: Comparison of experiment and theory for Ga_{17}^+ and Ga_{20}^+," Phys. Rev. B **73**(4), 045406 (2006).
[66]N. Drebov, F. Weigend, and R. Ahlrichs, "Structures and properties of neutral gallium clusters: A theoretical investigation," J. Chem. Phys. **135**(4), 044314 (2011).
[67]L. Sai, J. Zhao, X. Huang, and J. Wang, "Structural evolution and electronic properties of medium-sized gallium clusters from *ab initio* genetic algorithm search," J. Nanosci. Nanotechnol. **12**(1), 132–137 (2012).
[68]K. G. Steenbergen, D. Schebarchov, and N. Gaston, "Electronic effects on the melting of small gallium clusters," J. Chem. Phys. **137**(14), 144307 (2012).